Heliyon 5 (2019) e02868

Contents lists available at ScienceDirect

Heliyon

journal homepage: www.heliyon.com

Research article

A chronic high-fat diet causes sperm head alterations in C57BL/6J mice

A. Funes [a,1], T.E. Saez Lancellotti [a,1], L.D. Santillan [b], M.C. Della Vedova [b], M.A. Monclus [a], M.E. Cabrillana [a], S.E. Gomez Mejiba [c], D.C. Ramirez [b,**], M.W. Fornes [a,*]

[a] LIAM, Andrology Research Laboratory from Mendoza, IHEM-CCT-CONICET, National University of Cuyo and University of Aconcagua, Mendoza, 5500, Argentina
[b] LETM, Laboratory of Experimental and Translational Medicine, IMIBIO-SL, CONICET, National University of San Luis, San Luis, 5700, Argentina
[c] LET, Laboratory of Experimental Therapeutics, IMIBIO-SL, CONICET, National University of San Luis, San Luis, 5700, Argentina

ARTICLE INFO

Keywords:
Cell biology
Immunology
Molecular biology
Proteins
Diet
Male fertility
Mouse model
Inflammation
Sperm-head morphology
Dietary fat
Oxidative stress

ABSTRACT

A chronic-positive energetic balance has been directly correlated with infertility in men, but the involved mechanisms remain unknown. Herein we investigated weather in a mouse model a chronic feeding with a diet supplemented with chicken fat affects sperm head morphology. To accomplish this, we fed mice for 16 weeks with either control food (low-fat diet, LFD) or control food supplemented with 22% chicken fat (high-fat diet, HFD). At the end of the feeding regimen, we measured: redox and inflammatory changes, cholesterol accumulation in testis and analyzed testicular morphological structure and ultra-structure and liver morphology. We found that the mice fed HFD resembled some features of the human metabolic syndrome, including systemic oxidative stress and inflammation, this group showed an increment in the following parameters; central adiposity (adiposity index: 1.07 ± 0.10 *vs* 2.26 ± 0.17), dyslipidemia (total cholesterol: 153.3 ± 2.6 *vs* 175.1 ± 8.08 mg/dL), insulin resistance (indirect Insulin resistance index, TG/HDL-c: 2.94 ± 0.33 *vs* 3.68 ± 0.15) and fatty liver. Increased cholesterol content measured by filipin was found in the testicles from HFD (fluorescence intensity increase to 50%), as well as an alteration of spermiogenesis. Most remarkably, a disorganized manchette-perinuclear ring complex and an altered morphology of the sperm head were observed in the spermatozoa of HFD-fed mice. These results add new information to our understanding about the mechanisms by which systemic oxidative stress and inflammation may influence sperm-head morphology and indirectly male fertility.

1. Introduction

Overweight and obesity are chronic and costly inflammatory diseases [1]. C57BL/6J mice fed with food enriched in chicken-derived fat show central adiposity, systemic oxidative stress/inflammation, insulin resistance, and liver steatosis resembling most of the key features of the human metabolic syndrome [2]. In recent years, our research team and other authors have described specific changes in spermatogenesis in fat-fed animals that lead to low sperm count and abnormal sperm morphology, among other changes [1, 2, 3, 4, 5, 6, 7, 8, 9]. Although obesity is known to be a chronic inflammatory disease that causes oxidative stress in several tissues including the testicle [10], its influence on the last stages of spermatogenesis (spermiogenesis stage) has not yet been accurately reported [11, 12, 13].

The shaping of the mammalian sperm head involves the elongation and condensation of the spermatid nucleus, associated with the transitory appearance of a microtubular complex called manchette that participates in the development of the acrosome [14, 15]. The manchette consists of a perinuclear ring (PR) with inserted microtubules, and is found underlying the marginal ring (MR) of the acroplaxome. The acroplaxome is a bent plate of actin filaments that surrounds the spermatid nucleus and anchors the developing acrosome [14]. During spermatid elongation, the two overlapping rings reduce their diameter to fit the decreasing diameter of the spermatid nucleus [4].

Alterations in spermiogenesis induce significant head defects in mammalian spermatozoa [14]. An abnormal shape of the sperm head could be induced by ectopic placement of the manchette microtubules [14, 15]. Sperm head malformations have been reported in rabbits and rodents fed with high-fat diets [3, 4, 7, 9].

We previously found that sperm defects were the result of a defective development of the acrosome-manchette complex related to increased testicular cholesterol in rabbits [6, 7, 15, 16]. However, it remains to be

* Corresponding author.
** Corresponding author.
E-mail addresses: ramirezlabimbiosl@ymail.com (D.C. Ramirez), mfornes@fcm.uncu.edu.ar (M.W. Fornes).
[1] Co-first authorship.

https://doi.org/10.1016/j.heliyon.2019.e02868
Received 24 May 2019; Received in revised form 14 August 2019; Accepted 12 November 2019

clarified which molecular changes cause structural and ultra-structural alterations during this stage and the consequent modifications in the shape of the sperm head.

Other studies have shown testicular alterations among the changes found in a mouse model similar to the metabolic syndrome [7, 8, 16].

Previously, we have developed a mouse model displaying many of the characteristics of human metabolic syndrome. However, to our knowledge, there are no studies linking chronic feeding with chicken fat, spermatogenesis, inflammatory status and possible consequences on male fertility. The objective of this work was to test whether the shape of the sperm head is affected during spermiogenesis in a mouse model chronically fed with a high-chicken fat diet as a result of a negative redox balance. To address the underlying mechanisms, we studied cholesterol accumulation, inflammation, and oxidative stress, along with histology and morphology of the sperm head.

2. Materials and methods

2.1. Animal model

Six-week-old male C57BL/6J mice were used in this study following our previous report [2]. All experiments were carried out according to a protocol approved by the Institutional Committee for Use of Animals in Research of the National University of San Luis (Protocol# B97/15) and followed the guidelines of the Guide for Care and Use of Laboratory Animals in Research (USNIH). Twelve mice were randomly grouped in two groups and kept at a temperature of 23 ± 3 °C with dark–light cycles of 12 h, food and water provided *ad libitum*, during 16 weeks. Mouse chow was purchased from GEPSA S.A. and contained 6% chicken-derived fat, 40.7% carbohydrates, and 24% protein. The HFD was prepared in our laboratory by adding 22% chicken-derived fat (Granja Tres Arroyos) [2]. The final composition and caloric value of both diets are shown in Supplementary Table 1. Food analyses were performed as we previously reported [2].

Body weight gain (g) was recorded once a week. Systolic (SBP) and diastolic (DBP) blood pressures were measured every 4 weeks with a non-invasive tail-cuff system by using a CODA Surgical Monitor (Kent Scientific Co. Connecticut, USA).

At the end of the feeding period, animals were fastened for 12 h and anesthetized with vapors of isofluorane. The epididymal fat depot was removed following a surgical procedure and weighed. In this paper, the weight of peri epididymal grease was used as a marker of lipid accumulation (Adiposity index). This epididymal grease weight was related to body weight following a previous paper (weight of epididymal fat pad (g)/body weight (g)] ×100 and shown as AI%; [2]).

2.2. Measurements of adipokines and lipids

On the last day, after 12 h of fasting and under anaesthesia, blood samples from the six mice of each experimental group were taken from the abdominal aorta and plasma was collected for biochemical analysis: Fasting glycemia, triglyceride (TG), total cholesterol (TC), and high-density lipoprotein cholesterol (HDL-c) were measured in at least three independent experiments using commercially available kits (Weiner Laboratories, Rosario, Argentina). Low-density lipoprotein cholesterol (LDL-c) was calculated as follows: LDL-c = [TC-TG/5]-HDL-c [17]. The atherogenic index was calculated using the following formula: TC(mg/dl)/HDL-c(mg/dl) [18]. As an indirect parameter of insulin resistance the TG/HDL-c index was calculated [19].

2.3. Antioxidants in serum

Total antioxidant capacity (TAC) in serum from the six mice of each experimental group was measured in at least three independent experiments by an improved method that measures the quenching of the 2,2′-azino-bis-(3-ethylbenzothiazoline- 6-sulfonic acid) radical cation ($ABTS^{\bullet+}$) by both lipophilic and hydrophilic antioxidants present in serum. Reduced glutathione (GSH) concentration in serum was measured using a commercially available kit (Biovision Inc.). Oxidized glutathione (GSSG) was measured as GSH after treatment of the sample with GSH reductase following the manufacturer's instructions. Thiol status in serum is shown as the GSH/GSSG ratio. Catalase (CAT) - and total glutathione peroxidase (GPx) - specific activities were measured as described using Aebi's (REF) and Flohe and Gunzler's (REF) methods, respectively. The results are expressed as international units per milligram of total proteins (IU/mg proteins) [2].

2.4. Markers of systemic oxidative stress

As a marker of protein oxidation, protein carbonyls were determined as previously reported, for the six mice of each experimental group and in at least three independent experiments, using an enzyme linked immunesorbent assay (ELISA) and the results are shown as nanomoles of carbonyl per milligram of total proteins (nmol/mg protein) [20]. Lipid peroxidation was measured spectrophotometrically by determining malondialdehyde (MDA) concentration as thiobarbituric acid-reactive substances (TBARS) at 535 nm, and results are shown as micromoles of MDA per milligram of total proteins (μmol MDA/mg protein) [21].

2.5. Markers of systemic inflammation

Nitrite and IL-6 concentrations were measured in serum from the six mice of each experimental group and in at least three independent experiments as markers of systemic inflammation. The concentration of nitrite in the serum was measured spectrophotometrically by using the Griess reagents [22]. The results were shown as nmol of nitrite per milligram of protein (nmol NO_2^-/mg protein). Serum leptin, adiponectin and IL-6 were measured using an enzyme-linked immune-sorbent assay (ELISA) kits following the manufacturer's instructions (BioVision Inc., Milpitas, CA).

2.6. Histology

Small tissue samples of liver and testicle were obtained, fixed and processed by routine histological techniques. Tissue sections of 5–6 μm thickness were stained with hematoxylin–eosin (H&E) or preserved for cholesterol/filipin staining [23, 24, 25]. Images were acquired using a Nikon 80i microscope. Some testicle samples were fixed with Bouin's fixative solution containing 2% v/v glutaraldehyde and processed for electron microscopy. Ultrathin sections were stained by lead-uranyl classical stain techniques and observed in Zeiss 902 electron microscope. All tissue sections were obtained from the six mice from each group and evaluated in at least three independent experiments.

2.7. Cholesterol staining

Testicle semi-thin sections from the six mice of each experimental group were incubated with 40 μl of filipin working solution (0.15 mM in PBS) during 60 min at room temperature (protected from light). Then samples were washed with PBS three times and immediately were mounted with antifade solution. Imaging was performed on an Olympus FV1000 confocal microscope (Olympus America Inc., Center Valley, PA, USA). Five microscopic fields of each section (n = 5) were chosen randomly for fluorescence intensity evaluation by ImageJ software (https://imagej.nih.gov/ij/) [25]. Simultaneously, it was recorded the same images by Nomarkis's differential interference contrast (DIC) [26].

2.8. Statistical analysis

Unless otherwise indicated, data are shown as mean values ± standard error of the mean (S.E.M.), with six mice from each group and from at least three independent experiments. All statistical comparisons were

performed using the Student's *t*-test for independent groups. Differences were considered statistically different when $p < 0.05$.

3. Results

3.1. General characteristics of the animal model

The body weight of the animals was similar at the beginning of the study (the initial weight of the mice used in this study was of 20 g), but after the 16-week feeding period HFD mice weight was greater than control animals. Epididymal fat depot was also significantly higher in HFD *vs* LFD mice, as well as adiposity index. No significant changes in blood pressure were observed between HFD and LFD animals. Basal glycemia was higher in the HFD group than in the LFD group, as well as total cholesterol, low-density lipoprotein and triglycerides. There was no difference between the HDL-c concentration and the atherogenic index between the two experimental groups. However, the indirect insulin resistance TG/HDL-c index was higher in the HFD when compared to the LFD group (Supplementary Table 2).

3.2. Redox and inflammatory profile

Systemic redox and inflammatory status were established by measuring changes in the antioxidant concentration and inflammation markers in serum of mice fed LFD or HFD for 16 weeks (Supplementary Table 3). Serum TAC was measured as a parameter of antioxidant content that may change by depletion of antioxidants due to increased detoxification of pro-oxidants and inflammation [18]. The serum TAC of HFD animals decreased more than that of the LFD group (Supplementary Table 3). In order to assess systemic non-enzymatic antioxidant defenses, the GSH/GSSG ratio was measured in serum. The GSH/GSSG relationship in the HFD mouse serum was lower than that of the LFD group ($p < 0.001$). To assess enzymatic antioxidants in serum, we measured the specific activity of CAT and GPx. Serum CAT and GPX activitieswere higher in the HFD group than in the LFD group ($p < 0.001$).

Lipid peroxidation, a marker of lipid oxidation, was measured as TBARS (Supplementary Table 3). Serum TBARS in animals from the HFD group increased more than in the LFD group ($p < 0.001$). Serum carbonyl concentration, a marker of protein oxidation, was also higher in HFD mice than in the LFD group.

As also shown in Supplementary Table 3, nitrites and IL-6 concentrations in serum from HFD were higher than LFD. However, HFD fed mice had increased leptin, but reduced adiponectin concentrations in serum. This serum profile of adipokines and IL-6 suggests a systemic inflammation and an insulin-desensitizing status.

3.3. Liver morphology

Morphological analysis of liver sections clearly indicated that the HFD fed mice had a severe hepatic steatosis [27] (Fig. 1), showing noticeable fat vacuoles in most liver cells (Fig. 1, inset B′, arrows). Instead, liver cells from LFD showed normal histo-architecture (Figs. 1 A and A′).

3.4. Effects of HFD on testicular morphological structure

Morphological analysis of the testicles showed that HFD-fed mice had anomalous testicular architecture compared to control animals (Fig. 2). The seminiferous epithelium was disorganized (Fig. 2C, #) showing a number of epithelial cells in an organization that appeared loosely arranged (Fig. 2B and F, dashed lines). Moreover, histological images of the seminiferous tubules of HFD-fed mice showed several empty areas (Fig. 2E, asterisks), and the interstitial tissue appeared enlarged with a noticeable increase in foamy cells, which accounts for lipid accumulation and localized inflammation (Fig. 2H and I, black arrows).

3.5. Cholesterol accumulation in testis

As we had previously observed in our hypercholesterolemic rabbit model [3, 4], an increase in the tissues cholesterol was observed under chronic feeding of C57BL/6J mice with an HFD (Fig. 3A). Filipin staining showed that the accumulation of cholesterol increased at all stages of seminiferous epithelial cells. The quantification of Filipin fluorescence intensity showed that the cholesterol content in the testes from HFD increased more than in the control group (Figs. 3A and B).

3.6. Alteration of spermiogenesis in HFD fed mice

In order to characterize spermatogenesis anomalies in HFD mice at the ultra-structural level, testicles of HFD and LFD mice were studied by transmission electron microscopy (TEM). Sertoli cells from both groups were well organized (data not shown). In contrast, spermatogenic cells that progress through the stages of spermiogenesis, from round cell to elongated cell, showed morphological alterations.

As depicted in Fig. 4, the spermatids of LFD mice showed the acrosomal granule centrally located, equidistant from both acrosomic edges (Fig. 4A). In contrast, cells from HFD-fed mice showed an enlarged acrosome with an eccentrically localized acrosomal granule, unequally distanced from the edges (Fig. 4D). Subsequently in the spermatogenesis process, head elongation in a slight curvilinear direction was observed in the spermatozoa of control mice (Fig. 4B), as expected in the case of

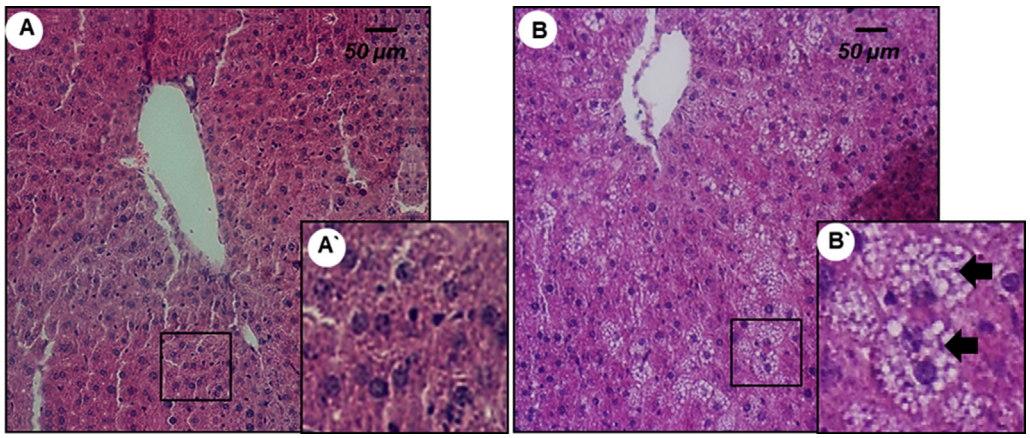

Fig. 1. HFD induced steatosis in C57BL/6J mice. H&E stained hepatic sections from LFD (A) and HFD (B) fed mice. Control mice show normal hepatocyte morphology with central nucleus and homogeneous eosinophilic cytoplasm (A′ insert) whereas HFD mice show hepatocytes with vacuolated cytoplasm (black arrows in B′). Magnification: A and B 250 X; A′ and B′ are three-fold enlarged images from A and B, respectively.

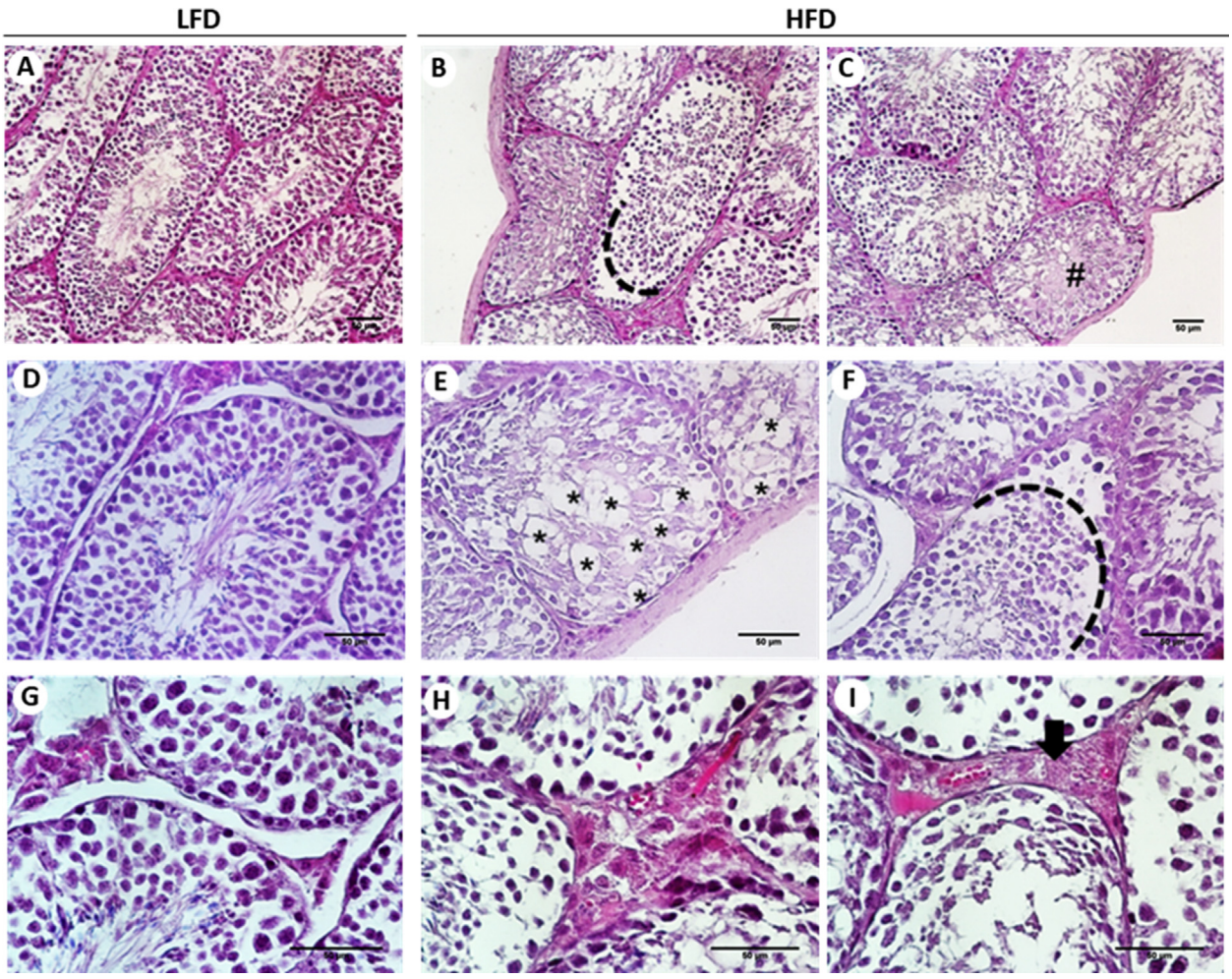

Fig. 2. HFD altered testicular morphology in C57BL/6J mice. Representative H&E images of LFD testicular tissue exhibit a normal histological morphology. Testicles from HFD mice show loosely arranged spermatogenic cells (dashed lines) on the seminiferous epithelium, epithelial disruption (#), vacuoles in the testis (*) and enlarged intersticium (black arrows). Magnification: A, B and C, 200 X; D, E and F, 400 X; and G, H and I, 600 X.

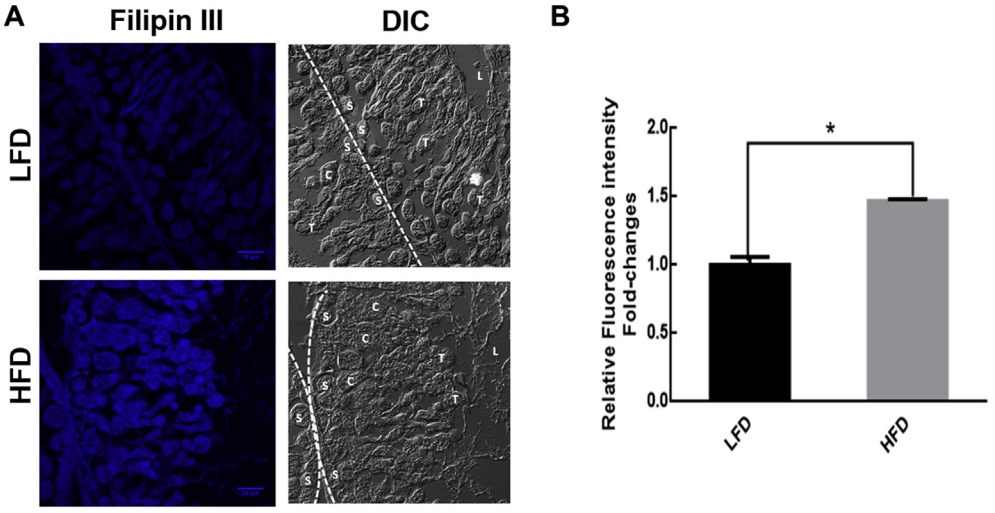

Fig. 3. HFD increased cholesterol content in seminiferous tubules of C57BL/6J mice. A. Representative fluorescence micrographs of LFD and HFD mice showing cholesterol content inside seminiferous tubules detected by the filipin III probe (left) and differential interference contrast (DIC) images (right) acquired at 600 X. L, lumen; S, spermatogonia; C. spermatocyte; T. spermatid. B. Densitometric Filipin III flurecensce image analysis. Filipin positive areas of seminiferous tubules is shown as mean ± SD, normalized to LFD (1), n = 5. Asterisk indicates $p < 0.05$.

sickle-shaped spermatozoa heads. On the other hand, a remarkably curved head was observed in the spermatozoa from HFD mice (Fig. 4E). This particular arrangement could be explained because the edges of the acrosome are not equatorially situated in HFD at this stage. Instead, one edge is placed ahead of the other, towards the future connection between the head and tail (arrows in Fig. 4B and E). The arrangement of these borders is thought to be species-specific, particularly for the sickle-shaped head of mouse sperm. The sperm-forming heads of HFD-fed

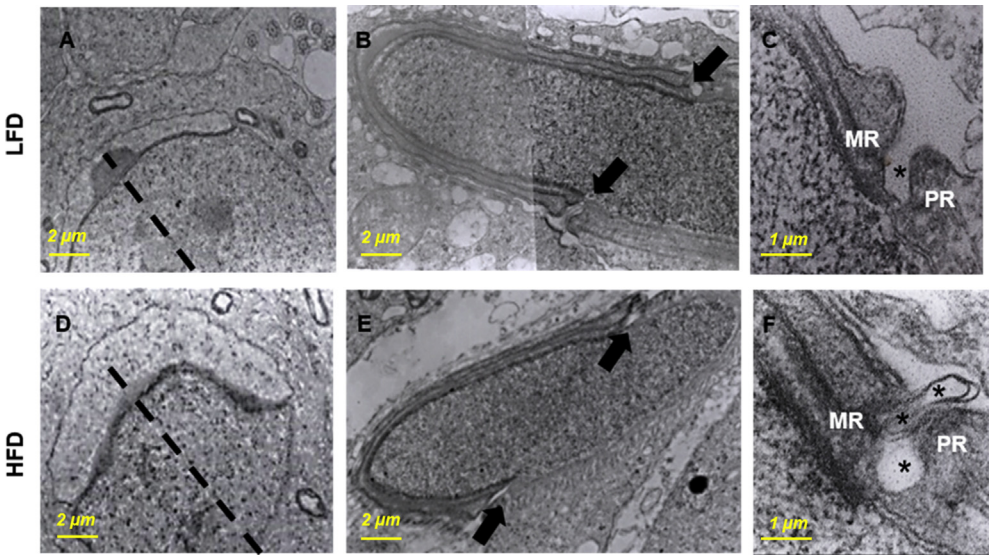

Fig. 4. HFD altered sperm acrosomal development in C57BL/6J mice. Representative transmition electron micrographs of seminiferous epithelium of mice fed either an LFD (A, B, C) or an HFD (D, E, F) for 16 weeks. A) Symmetrical and D) asymmetrical expansion of acrosomal vesicle from Golgi granule (the central axis is delineated by dashed lines), elongation of both acrosomal edges (arrows in B and E) and circumferential border (C and F; MR: marginal ring, PR: perinuclear ring, *: circumferential groove). Magnification: A, B, D and E, 18000 X; C and F, 32000 X.

mice, however, showed an abnormal (greater) distance between the two edges (black arrows in Fig. 4E).

In control mice, perinuclear ring (PR) of the manchette was placed adjacent to the marginal ring (MR) of the acroplaxome and a peri-nuclear groove marks the acroplaxome-manchette boundary (Fig. 4C, asterisk). However, in sperm cells from HFD mice these structures showed a visibly disorganized architecture (Fig. 4F). Both rings lost their normal arrangement, and the groove was found anomalous and displaced.

4. Discussion

Here we use a mouse model to test whether a chronic fat diet causes changes in the morphology of the sperm head, which may affect fertility function. To achieve this aim, we used our previously characterized experimental model of mice fed HDF or LFD for 16 weeks. To our best understanding, we show for the first time that chronic feeding with a HFD caused sperm head alterations as assessed by histological and ultrastructural analyses, along with systemic oxidative stress/inflammation and fatty liver histological pattern.

The number of studies relating obesity to alterations in the parameters of spermiogenesis has begun to increase exponentially due to the low fertility observed in overweight and obese men [9, 28]. Recently, we informed that hypercholesterolemic rabbits showed sperm head defects under a HFD [3, 4]. These spermatogenic defects were prevented by reducing dietary fat and supplementing with olive oil [4, 29]. This and other evidences [1, 13, 30] suggest that systemic oxidative stress and inflammation may play a key role in the accumulation of cholesterol in the testicles, as well as cytoskeleton disorganization during spermiogenesis.

The diet-induced obesity mouse model used in this study was successfully established by feeding C57BL/6J mice with a diet enriched in 22%v/w chicken fat during 16 weeks. Compared to control, mice fed HFD showed higher body weight gain, increased adiposity, total cholesterol, TG and LDL-c concentrations in the plasma and fatty liver [2]. These animals also showed systemic inflammation/oxidative stress and insulin resistance.

High serum leptin in this model is related to the obese condition. Moreover, leptin is reported to modulate human Sertoli cells [31]. In this sense, human Sertoli cells dramatically decrease the production of acetate under leptin increasing [32]. In this particular case, the Sertoli cell exerts a high influence on spermiogenesis and therefore some effect should not be ruled out. Adiponectin's effects on spermatozoa seem to be beneficial, as it was stated for lean men, although it is difficult to attribute to a cytokine a specific change in the spermiogenesis process.

Adiposity and associated pro-inflammatory status in male mice can induce testicular inflammation through activating several different signaling pathways [33]. This contributes to the deregulation of spermatogenesis and other functions of testicular cells [28, 34, 35]. Accordingly, our results indicate that chronic feeding of mice with a diet supplemented with chicken fat can cause systemic oxidative stress and inflammation, as well as a regional inflammatory reaction in the male genital tract, where the microenvironment is essential to support sperm production and function [7]. It is also known that systemic inflammation can damage the male genital tract by increasing the generation of reactive oxygen species by innate immune cells that infiltrate the seminiferous epithelium [36, 37, 38]. Consequently, the pattern of systemic oxidative stress/inflammation and dyslipidemia, as shown in this study, could affect normal morphology of the sperm head.

An altered mammalian spermiogenesis affects fertility by causing pleiotropic-head defects during spermatozoa production [37]. An abnormal head shape can be caused by an anomalous shape of the nucleus due to the ectopic position of the manchette's microtubules [39]. This probably causes an alteration in the anchorage of the microtubules (as seen in rabbits), which probably results in the abnormal shape of the sperm heads [4, 29].

Several authors have reported sperm malformations in this and other diet-induced obesity models [3, 7, 9]. However, it remains unclear what molecular changes lead to structural and ultra-structural changes during acrosomic development [4]. Interestingly, our results indicate that an increase in the accumulation of cholesterol in the testicles of mice fed HFD might be the cause of structural changes and altered sperm heads [3, 4, 40]. This high cholesterol concentration could modify the lipid-protein arrangement that characterizes raft membranes, which would eventually modify the function of the microdomains [4, 40]. During spermatogenesis, it is not well understood at present how the microtubules of the manchette bind to the lipids of the membrane. However, the actin filaments and their regulating proteins, which act as a bridge between microdomains and microtubules, are probably involved [14]. Indeed, the correct disposition of lipids seems to be crucial for the accurate functioning and location of the manchette. The accumulation of cholesterol in the testicles and the altered organization of the manchette are therefore responsible for the altered shape of the sperm and the consequent lack of fertility capacity.

In conclusion, our results indicate that a chronic feeding with a diet supplemented with chicken fat causes systemic inflammation/oxidative stress, dyslipidemia, fatty liver and an altered spermiogenesis. In this

study, we provide evidence that the alterations in spermiogenesis involve an increase in cholesterol in the membrane and disorganization of the manchette, resulting in an alteration in the morphology of the sperm head. Such a scenario may eventually damage the fertility functions of mature gametes in obese humans. Greater effort must be made to establish the molecular mechanisms involved in fat-induced alterations in sperm shape and quality, but it certainly involves cell membrane cholesterol and manchette dysfunction.

Declarations

Author contribution statement

Funes A: Performed the experiments; Wrote the paper.

Saez Lancellotti TE, Gomez Mejiba SE, Ramirez DC, Fornes MW: Conceived and designed the experiments; Analyzed and interpreted the data; Wrote the paper.

Santillan L.D., Della Vedova MC: Performed the experiments.

Monclus MA, Cabrillana ME: Contributed reagents, materials, analysis tools or data.

Funding statement

This work was supported by the Program from SECTyP, National University of Cuyo; CIUDA, University of Aconcagua, Argentina and by the Agencia Nacional para la Promoción de la Ciencia y la Tecnología-FONCyT, Argentina (PICT-2014-3369), Universidad Nacional de San Luis, Argentina (PROICO 02-3418 to DCR, PROICO 10-0218), and the CONICET (PIP-916).

Competing interest statement

The authors declare no conflict of interest.

Additional information

Supplementary content related to this article has been published online at https://doi.org/10.1016/j.heliyon.2019.e02868.

References

[1] W. Fan, et al., Obesity or overweight, a chronic inflammatory status in male reproductive system, leads to mice and human subfertility, Front. Physiol. 8 (2017) 1117.
[2] M.C. Della Vedova, et al., A mouse model of diet-induced obesity resembling most features of human metabolic syndrome, Nutr. Metab. Insights 9 (2016) 93–102.
[3] T.E. Saez Lancellotti, et al., Hypercholesterolemia impaired sperm functionality in rabbits, PLoS One 5 (10) (2010) e13457.
[4] L. Simon, et al., Manchette-acrosome disorders during spermiogenesis and low efficiency of seminiferous tubules in hypercholesterolemic rabbit model, PLoS One 12 (2) (2017), e0172994.
[5] B.I. Ghanayem, et al., Diet-induced obesity in male mice is associated with reduced fertility and potentiation of acrylamide-induced reproductive toxicity, Biol. Reprod. 82 (1) (2010) 96–104.
[6] B.C. Borges, et al., Obesity-induced infertility in male mice is associated with disruption of Crisp4 expression and sperm fertilization capacity, Endocrinology 158 (9) (2017) 2930–2943.
[7] Y. Fan, et al., Diet-induced obesity in male C57BL/6 mice decreases fertility as a consequence of disrupted blood-testis barrier, PLoS One 10 (4) (2015), e0120775.
[8] Y. Mu, et al., Diet-induced obesity impairs spermatogenesis: a potential role for autophagy, Sci. Rep. 7 (2017) 43475.
[9] A. Pushpendra, G.C. Jain, Hyper-lipidemia and male fertility: a critical review of literature, Andrology (Los Angel) 4 (2) (2015).
[10] J. Zhao, et al., Leptin level and oxidative stress contribute to obesity-induced low testosterone in murine testicular tissue, Oxid. Med. Cell Longev. 2014 (2014) 190945.
[11] O. Rufus, O. James, A. Michael, Male obesity and semen quality: any association? Int. J. Reprod. Biomed. (Yazd) 16 (4) (2018) 285–290.
[12] J. Ma, et al., Association between BMI and semen quality: an observational study of 3966 sperm donors, Hum. Reprod. 34 (1) (2019) 155–162.
[13] G.L. Veron, et al., Impact of age, clinical conditions, and lifestyle on routine semen parameters and sperm kinematics, Fertil. Steril. 110 (1) (2018) 68–75 e4.
[14] A.L. Kierszenbaum, E. Rivkin, L.L. Tres, Molecular biology of sperm head shaping, Soc. Reprod. Fertil. Suppl. 65 (2007) 33–43.
[15] A.L. Kierszenbaum, E. Rivkin, L.L. Tres, Cytoskeletal track selection during cargo transport in spermatids is relevant to male fertility, Spermatogenesis 1 (3) (2011) 221–230.
[16] J.L. Zhao, Y.Y. Zhao, W.J. Zhu, A high-fat, high-protein diet attenuates the negative impact of casein-induced chronic inflammation on testicular steroidogenesis and sperm parameters in adult mice, Gen. Comp. Endocrinol. 252 (2017) 48–59.
[17] M.I.D. Marvin Querales, Susan Rojas, *Estimación del colesterol LDL a través de la ecuación brasilera: comparación con otras metodologías*, Rev. Latinoam. Patol. Clín. Med. Lab. 62 (2) (2015) 91–96.
[18] U.I. Nwagha, et al., Atherogenic index of plasma as useful predictor of cardiovascular risk among postmenopausal women in Enugu, Nigeria, Afr. Health Sci. 10 (3) (2010) 248–252.
[19] K.A. Young, et al., The triglyceride to high-density lipoprotein cholesterol (TG/HDL-C) ratio as a predictor of insulin resistance, beta-cell function, and diabetes in Hispanics and African Americans, J. Diabet. Complicat. 33 (2) (2019) 118–122.
[20] C.C. Winterbourn, I.H. Buss, Protein carbonyl measurement by enzyme-linked immunosorbent assay, Methods Enzymol. 300 (1999) 106–111.
[21] H.H. Draper, M. Hadley, Malondialdehyde determination as index of lipid peroxidation, Methods Enzymol. 186 (1990) 421–431.
[22] T. Wada, et al., Spironolactone improves glucose and lipid metabolism by ameliorating hepatic steatosis and inflammation and suppressing enhanced gluconeogenesis induced by high-fat and high-fructose diet, Endocrinology 151 (5) (2010) 2040–2049.
[23] K.L. Ma, et al., Inflammatory stress induces lipid accumulation in multi-organs of db/db mice, Acta Biochim. Biophys. Sin. 47 (10) (2015) 767–774.
[24] Z.B. Hu, et al., Activation of the CXCL16/CXCR6 pathway by inflammation contributes to atherosclerosis in patients with end-stage renal disease, Int. J. Med. Sci. 13 (11) (2016) 858–867.
[25] K.L. Ma, et al., Lipoprotein(a) accelerated the progression of atherosclerosis in patients with end-stage renal disease, BMC Nephrol. 19 (1) (2018) 192.
[26] I. Freitas, et al., In situ detection of reactive oxygen species and nitric oxide production in normal and pathological tissues: improvement by differential interference contrast, Exp. Gerontol. 37 (4) (2002) 591–602.
[27] W. Liang, et al., Establishment of a general NAFLD scoring system for rodent models and comparison to human liver pathology, PLoS One 9 (12) (2014), e115922.
[28] S.S. Deshpande, et al., Genetically inherited obesity and high-fat diet-induced obesity differentially alter spermatogenesis in adult male rats, Endocrinology 160 (1) (2019) 220–234.
[29] L. Simon, et al., Manchette-acrosome disorders and testicular efficiency decline observed in hypercholesterolemic rabbits are recovered with olive oil enriched diet, PLoS One 13 (8) (2018), e0202748.
[30] A. Agarwal, K. Makker, R. Sharma, Clinical relevance of oxidative stress in male factor infertility: an update, Am. J. Reprod. Immunol. 59 (1) (2008) 2–11.
[31] M.G. Alves, et al., Male fertility and obesity: are ghrelin, leptin and glucagon-like peptide-1 pharmacologically relevant? Curr. Pharmaceut. Des. 22 (7) (2016) 783–791.
[32] A.D. Martins, et al., Leptin modulates human Sertoli cells acetate production and glycolytic profile: a novel mechanism of obesity-induced male infertility? Biochim. Biophys. Acta 1852 (9) (2015) 1824–1832.
[33] M. Maegawa, et al., A repertoire of cytokines in human seminal plasma, J. Reprod. Immunol. 54 (1-2) (2002) 33–42.
[34] Y.F. Jia, et al., Obesity impairs male fertility through long-term effects on spermatogenesis, BMC Urol. 18 (1) (2018) 42.
[35] M. Fraczek, M. Kurpisz, Cytokines in the male reproductive tract and their role in infertility disorders, J. Reprod. Immunol. 108 (2015) 98–104.
[36] B.J.M. Mayorga-Torres, et al., Are oxidative stress markers associated with unexplained male infertility? Andrologia 49 (5) (2017).
[37] R.J. Aitken, Reactive oxygen species as mediators of sperm capacitation and pathological damage, Mol. Reprod. Dev. 84 (10) (2017) 1039–1052.
[38] C. Keck, et al., Seminal tract infections: impact on male fertility and treatment options, Hum. Reprod. Update 4 (6) (1998) 891–903.
[39] S.S. Du Plessis, et al., The effect of obesity on sperm disorders and male infertility, Nat. Rev. Urol. 7 (3) (2010) 153–161.
[40] M.G. Buffone, et al., High cholesterol content and decreased membrane fluidity in human spermatozoa are associated with protein tyrosine phosphorylation and functional deficiencies, J. Androl. 30 (5) (2009) 552–558.